Supplementary Information to:

Phosphatidylinositol 4,5-bisphosphate clusters act as molecular beacons for vesicle recruitment

Alf Honigmann[1*], Geert van den Bogaart[2,3*], Emilio Iraheta[4], H. Jelger Risselada[5], Dragomir Milovanovic[2], Veronika Mueller[1], Stefan Müllar[6], Ulf Diederichsen[6], Dirk Fasshauer[4], Helmut Grubmüller[5], Stefan W. Hell[1], Christian Eggeling[1,7], Karin Kühnel[2], Reinhard Jahn[2]

1- Department of Nanobiophotonics, Max Planck Institute for Biophysical Chemistry, Göttingen, Germany
2- Department of Neurobiology, Max Planck Institute for Biophysical Chemistry, Göttingen, Germany
3- Department of Tumor Immunology, Radboud University Nijmegen Medical Centre, Nijmegen, The Netherlands
4- Faculty of Biology and Medicine, University of Lausanne, Lausanne, Switzerland
5- Department of Theoretical and Computational Biophysics, Max Planck Institute for Biophysical Chemistry, Göttingen, Germany
6- Institute for Organic and Biomolecular Chemistry, Georg-August-University Göttingen, Göttingen, Germany
7- Weatherall Institute of Molecular Medicine, University of Oxford, Oxford, UK

*Both authors contributed equally to this work.

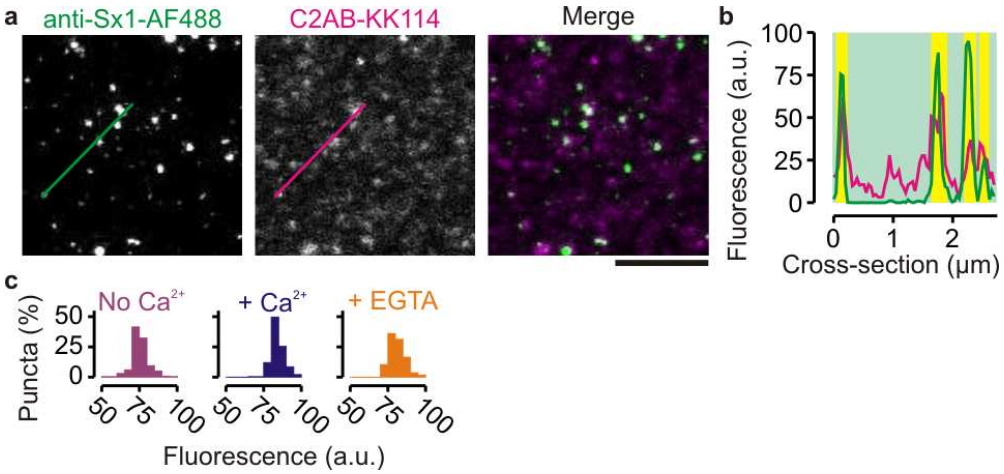

Supplementary Figure 1. Synaptotagmin-1 binding to syntaxin-1 clusters in membrane sheets derived from PC12 cells analyzed by two-color STED microscopy. (**a**) Representative STED images of PC12 membrane sheets (fixed in 4% (w/v) paraformaldehyde) stained with a combination of HPC-1 (against syntaxin-1; 2 µg/ml) and a secondary immunoglobulin G conjugated to Alexa fluor 488 (Invitrogen, A10680; 1:100 (v/v) dilution; anti-Sx1-AF488; green, left) and 100 nM of C2AB labeled with KK114 (C2AB-KK114; magenta, middle). Immunostaining was performed as described[7]. C2AB clustering was more pronounced in unfixed than in fixed membrane sheets (see Fig. 1). (**b**) Fluorescence intensity profiles through the lines marked in **a** (see Fig. 1), indicating an overlap of C2AB and syntaxin-1A clusters, *i.e.* C2AB bound to the syntaxin-1A clusters in absence of Ca^{2+}. (**c**) Histogram showing the distributions of C2AB binding to the puncta from figure 1g. (scale bars, 2 µm)

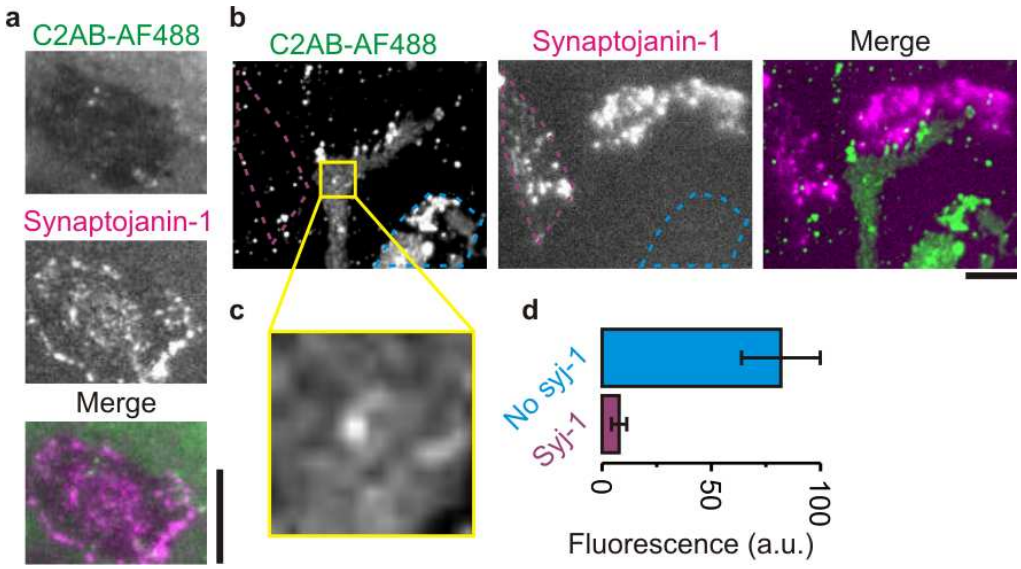

Supplementary Figure 2. Overexpression of a membrane-targeted variant of the PIP2-phosphatase synaptojanin-1 strongly reduced binding of synaptotagmin-1 to the plasma membrane. (**a**) Representative epi-fluorescence images of a PC12 membrane sheet in the absence of Ca^{2+} incubated with 100 nM C2AB labeled with Alexa fluor 488 (C2AB-AF488; top, green) and expressing the PIP2-phosphatase synaptojanin-1 (middle, magenta). The contrast of the green channel is enhanced to accentuate the lack of C2AB-AF488 binding to the membrane sheet. (**b**) Same as **a**, but now in presence of 200 µM Ca^{2+} and several sheets expressing different levels of the PIP2-phosphatase synaptojanin-1 (middle, magenta). Purple and cyan dotted lines mark membrane sheets over- or non-expressing synaptojanin-1, respectively. (**c**) Magnification of the region indicated in **b** from a membrane sheet non-expressing synaptojanin-1 showing the punctate binding of C2AB (see also Fig. 1a). (**d**) Quantification of the green (C2AB-AF488) fluorescence per sheet from **b**. Intensities were averaged over the entire area of the membrane sheets and expressed as counts per pixel (Syj-1, purple: overexpressed; No syj-1, cyan: non-transfected). Error bars show s.e.m. from at least 16 cells. Overexpression of the synaptojanin-1 construct completely removed PIP2 from the membrane[7,30] and reduced both Ca^{2+}-independent and Ca^{2+}-dependent membrane binding of C2AB-AF488. Membrane sheets were imaged by epi-fluorescence microscopy with the following filters: C2AB-AF488: 480/40 | 505LP | 527/50; synaptojanin-1-RFP: 565/30 | 590LP | 645/35 (excitation | dichroic | emission; all from Zeiss). (scale bars, 10 µm)

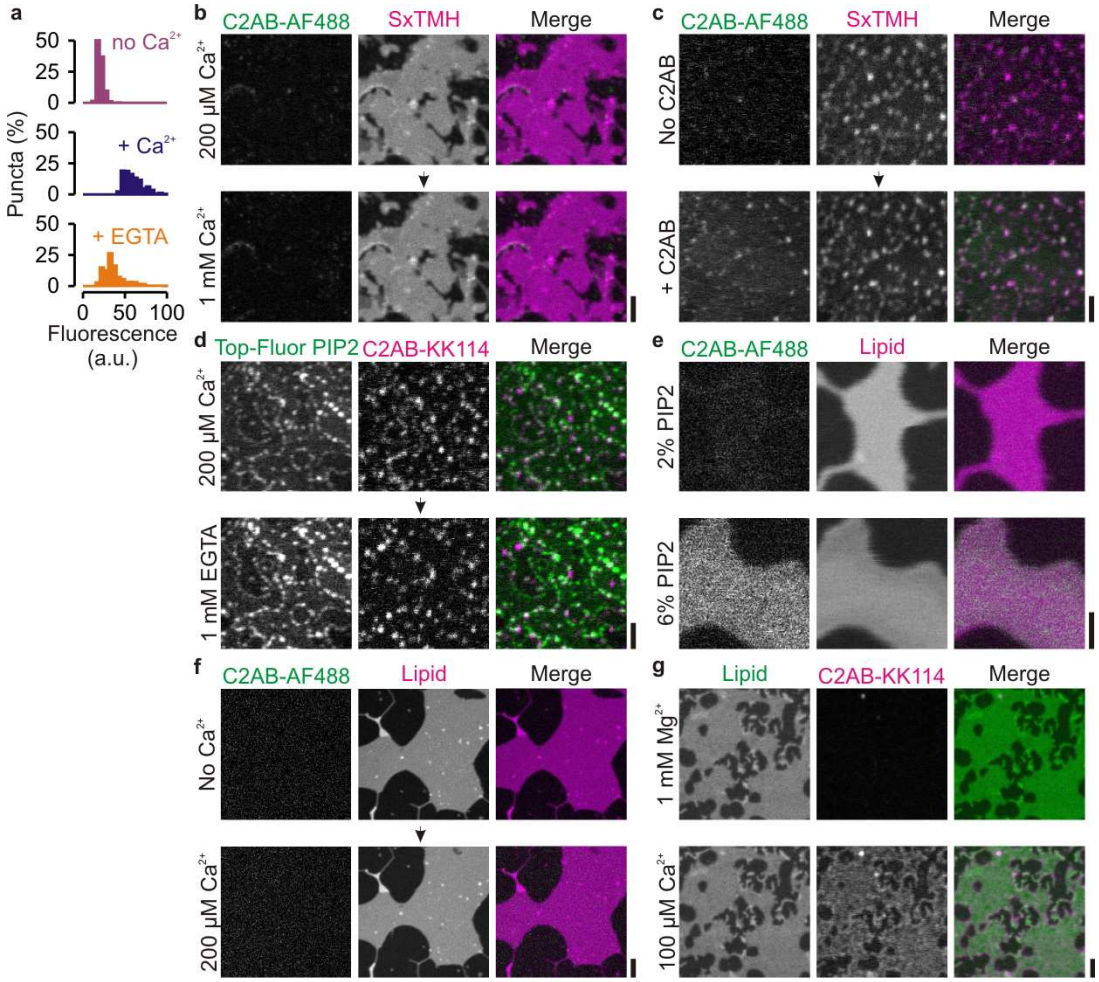

Supplementary Figure 3. Control experiments with supported lipid bilayers. (**a**) Histogram showing the distributions of C2AB binding to the puncta from figure 4d. (**b**) Representative confocal images of supported lipid bilayers lacking PS and PIP2 (70% DOPC, 30% cholesterol) and containing a fragment of syntaxin-1A (syntaxin-$1A_{257-288}$) encompassing the transmembrane domain and the polybasic linker, labeled with Atto647N (SxTMH; magenta). No clustering of SxTMH and no binding of labeled C2AB (C2AB-AF488; green) was observed. (**c**) Representative confocal images of supported lipid bilayers containing PS and PIP2 (46% DOPC, 30% cholesterol, 20% DOPS, 4% PIP2) and SxTMH (magenta). C2AB-AF488 bound to the SxTMH clusters despite of the presence of DOPS and independent of Ca^{2+}. (**d**) Representative confocal images of supported lipid bilayers containing labeled PIP2 (0.1% Top-Fluor PIP2; green) and unlabeled SxTMH (69% DOPC, 30% cholesterol, 1% PIP2). C2AB (C2AB-KK114; magenta) bound to the PIP2 clusters independent of Ca^{2+}. (**e**) Representative confocal images of supported lipid bilayers containing increasing PIP2 concentrations (DOPC with 2 – 6% PIP2), doped with labeled PE (0.1 mol% Atto647N-PE; Lipid, magenta) for visualization. In absence of Ca^{2+}, C2AB-AF488 (green) bound to membranes containing 6 mol% PIP2 but not 2 mol% PIP2. (**f**) Same as **e**, but now in absence of PIP2. C2AB did not bind to supported lipid bilayers, regardless of the presence of Ca^{2+}. (**g**) Representative confocal images of supported lipid bilayers containing PIP2 (98% DOPC, 2% PIP2) and a fluorescent lipid analog (0.1 mol% bodipy-FL PE, green) for visualization and in the presence of 1 mM Mg^{2+} and 100 µM Ca^{2+}. Mg^{2+} did not result in binding of C2AB-KK114 (magenta), whereas addition of Ca^{2+} did. (scale bars, 2 µm)

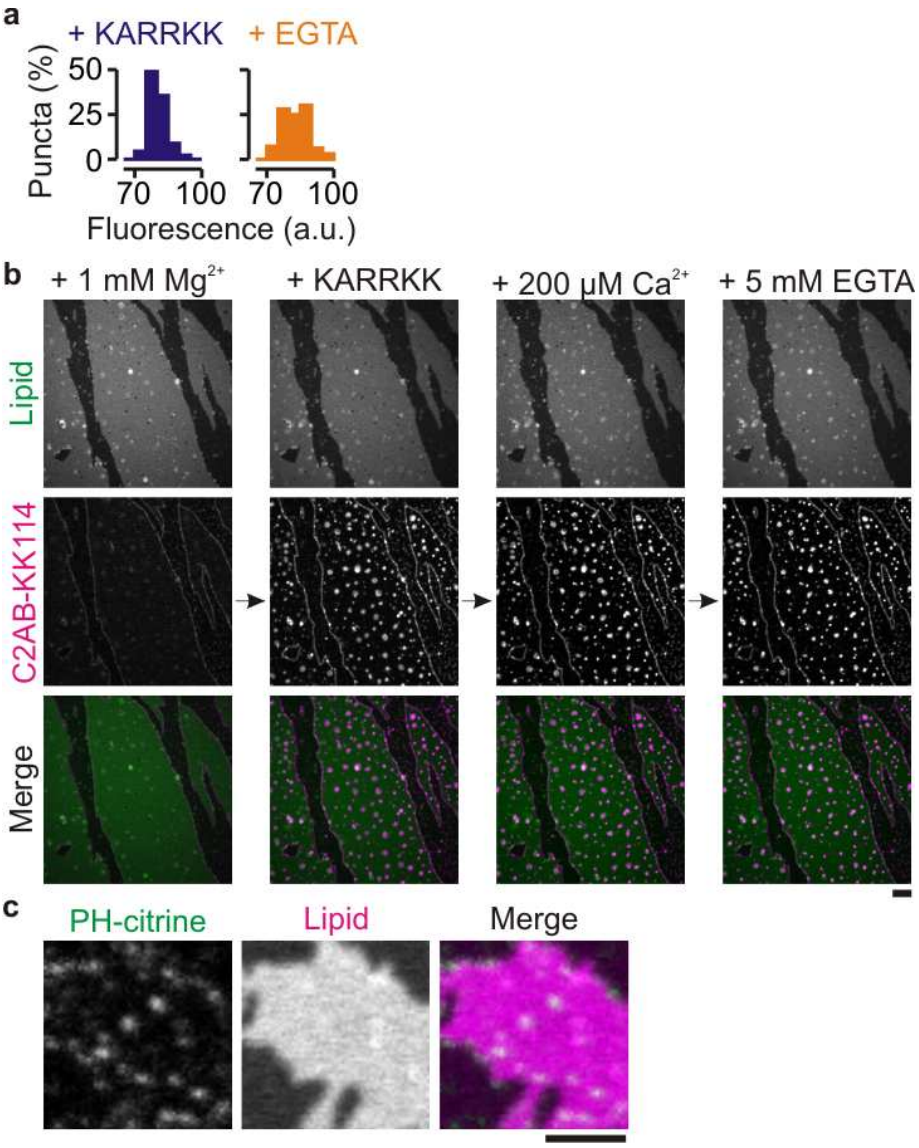

Supplementary Figure 4. Clustering of bound synaptotagmin-1 in model membranes containing PIP2 and the polybasic linker region of syntaxin-1A (^{260}KARRKK^{265}) is independent of Ca^{2+} and Mg^{2+}. (**a**) Histogram showing the distributions of C2AB binding to the puncta from figure 5d. (**b**) Representative confocal images of supported lipid bilayers (98% DOPC, 2% PIP2) with 0.1 mol% bodipy-FL PC as a lipid marker (Lipid, green) and C2AB labeled with KK114 (C2AB-KK114; magenta). Addition of ^{260}KARRKK^{265} to a final concentration of 20 µM induced membrane binding and clustering of C2AB. Cluster formation was not affected when $Mg^{2+}$was added at a final concentration of 1 mM. The clusters were also not affected by addition of 200 µM Ca^{2+} or by addition of 5 mM EGTA. (**c**) Representative confocal images as in panel **b**, but now with Atto647N-PE as lipid marker (Lipid, magenta) and with the PH-domain of phospholipase C delta fused to citrine (PH-citrine; green; see reference (7) for experimental details). PH-citrine bound to the domains induced by ^{260}KARRKK^{265}, indicating the presence of PIP2 in these domains. (scale bars, 2 µm)

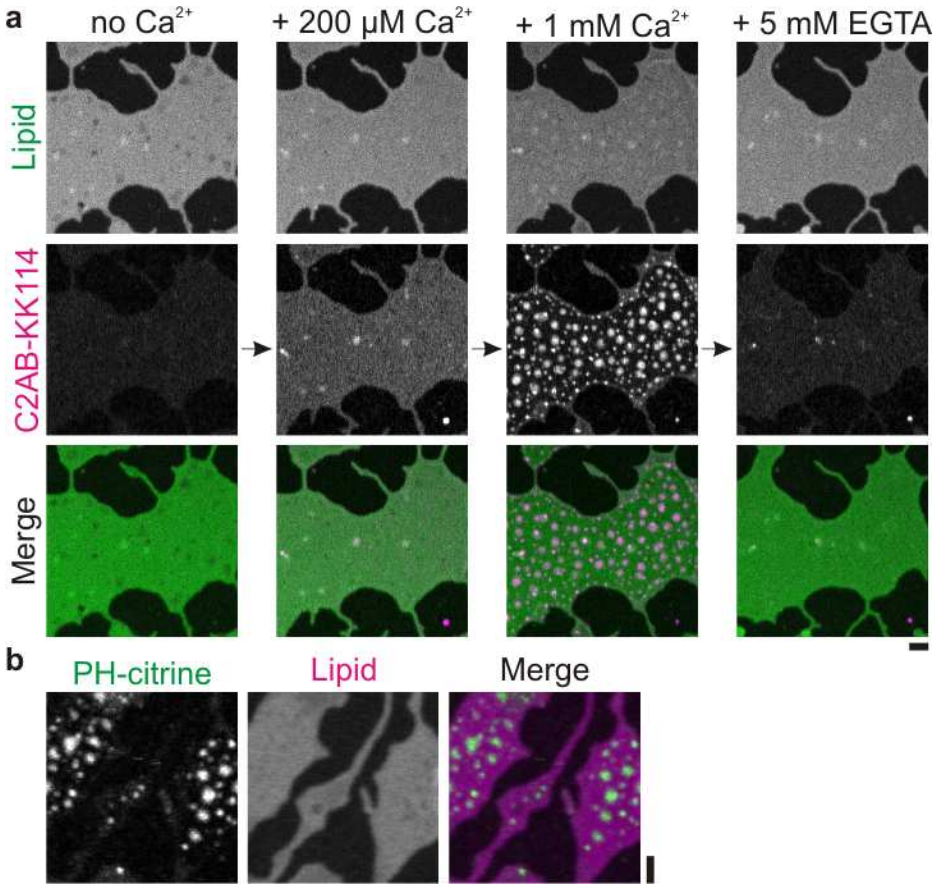

Supplementary Figure 5. PIP2 clustering in model membranes induced by 1 mM Ca^{2+} without syntaxin-1. (**a**) Representative confocal images of C2AB labeled with KK114 (C2AB-KK114; magenta) binding to supported lipid bilayers (98% DOPC, 2% PIP2) with 0.1 mol% bodipy-FL PC as a lipid marker (Lipid, green). C2AB did not bind to the membrane without Ca^{2+} (left), but binding was induced by addition of Ca^{2+} to a final concentration of 200 µM (middle left). Further addition of Ca^{2+} (1 mM) induced PIP2 clustering (as reported previously[34]) with C2AB bound to these clusters. These clusters could (in contrast to the Ca^{2+}-independent syntaxin-1 induced clusters in Supp. Fig. 4) be fully reversed by addition of an excess of 5 mM of the Ca^{2+}-chelator EGTA. (**b**) Representative confocal images as in panel **a**, but now with Atto647N-PE as lipid marker (Lipid, magenta) and with the PH domain of phospholipase C delta fused to citrine (PH-citrine; green; see reference (7) for experimental details). PH-citrine bound to the domains induced by Ca^{2+}, indicating the presence of PIP2 in these domains. (scale bars, 2 µm)

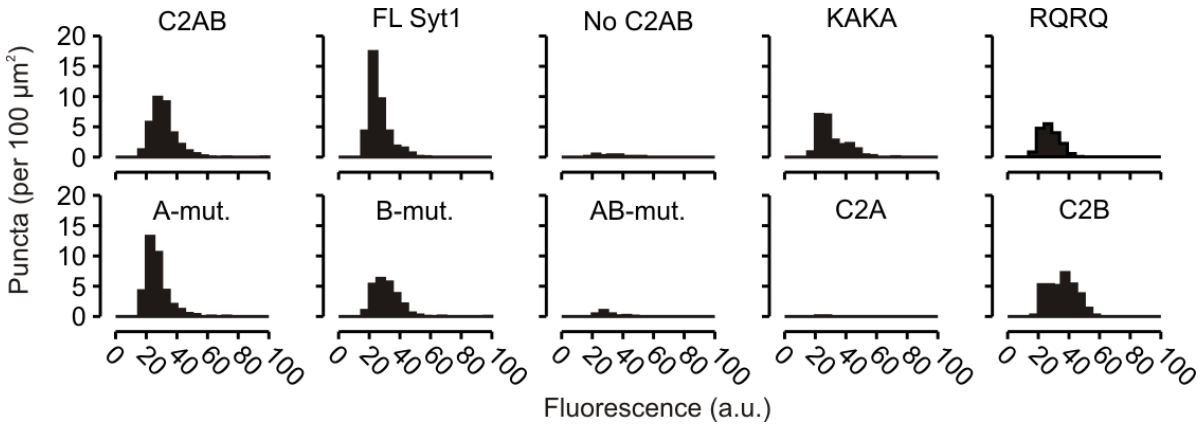

Supplementary Figure 6. Histograms showing the fluorescence intensity distributions of the puncta (per 100 μm^2) from the liposome binding experiment shown in figure 7b.

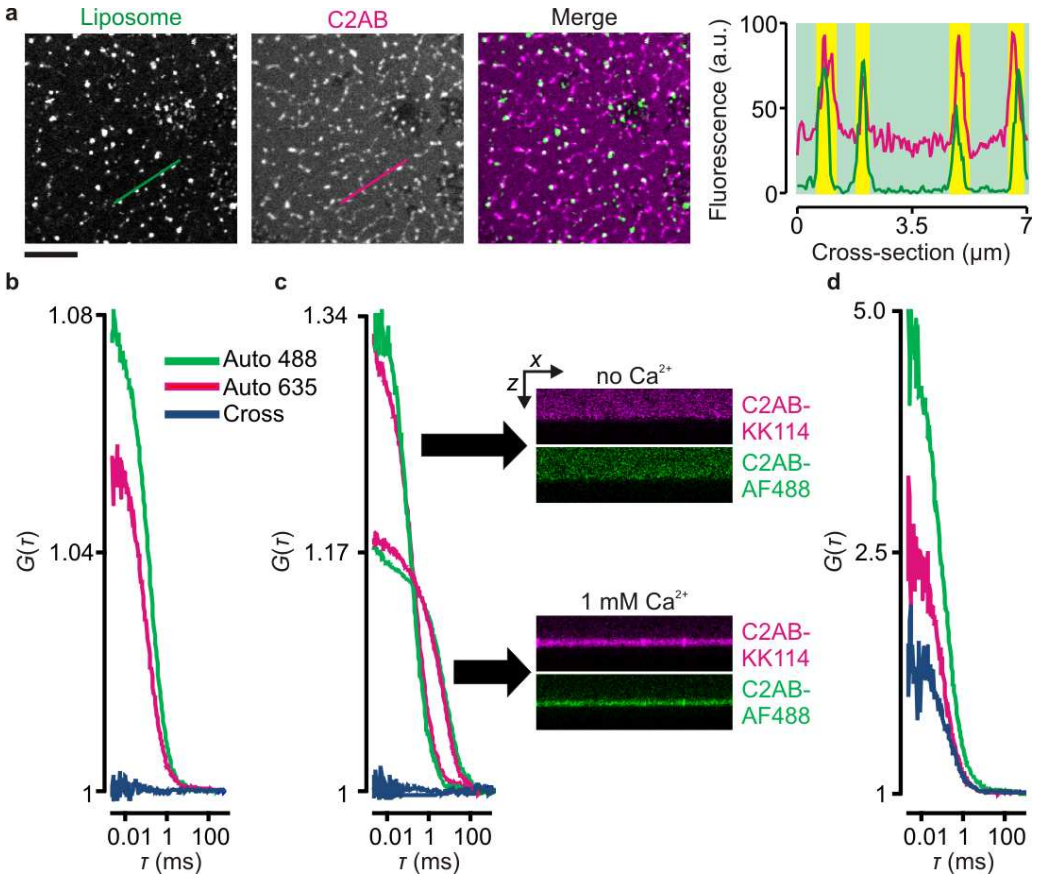

Supplementary Figure 7. The C2AB-fragment did not oligomerize under our experimental conditions. (**a**) Recruitment of liposomes to supported bilayers containing C2AB bound to syntaxin–PIP2 clusters. The experiment was carried out as in figure 7a, except that unbound C2AB was thoroughly washed away prior to addition of the liposomes. Liposomes were still recruited to C2AB enriched membrane clusters, excluding that C2AB needs to be pre-bound to both membranes for liposome tethering (compare to reference (20)). (**b**) Fluorescence cross correlation spectroscopy in a solution containing ~30 nM of each C2AB labeled with Alexa fluor 488 (green curves; Auto 488) and C2AB labeled with KK114 (magenta curves; Auto 635) and in presence of 1 mM Ca^{2+}. Blue curves: cross correlation (Cross). (**c**) Same as panel **b**, but now with ~7 nM of each C2AB-AF488 and C2AB-KK114 and in the presence of a supported lipid bilayer (85% DOPC, 15% DOPS). The confocal spot was positioned on the membrane. The insets show orthogonal views of the sample (*x*-*z*). In absence of Ca^{2+} (upper curves), C2AB did not bind to the supported lipid bilayer. Upon addition of 1 mM Ca^{2+}, the majority (~93%) of C2AB bound to the membranes and the diffusion coefficient of C2AB decreased from D = 79 µm^2 s^{-1} in absence of Ca^{2+} to D = 4.4 µm^2 s^{-1} in presence of 1 mM Ca^{2+}. This decreased diffusion coefficient is comparable to the mobility of fluorescent phospholipid analogues[29]. Membrane binding of C2AB was also apparent from the increased fluorescence at the membrane interface after addition of Ca^{2+} (compare *x*-*z* images of the membrane region). Importantly, we did not observe significant cross-correlation under any applied condition (in solution or membrane-bound and with or without Ca^{2+}), which indicates that the major fraction of the C2AB population diffused as monomers. (**d**) Positive control for cross-correlation. To determine the maximum overlap of the focal volumes for the two channels (488 and 635 nm), we measured FCCS in a solution (*i.e.* in the absence of a membrane) containing 0.5 nM of double-labeled double-stranded DNA (IBA, Göttingen Germany). The results for the FCCS standard probe gave high cross-correlation amplitudes verifying the alignment of the setup. Full experimental details are in the Supplementary Notes.

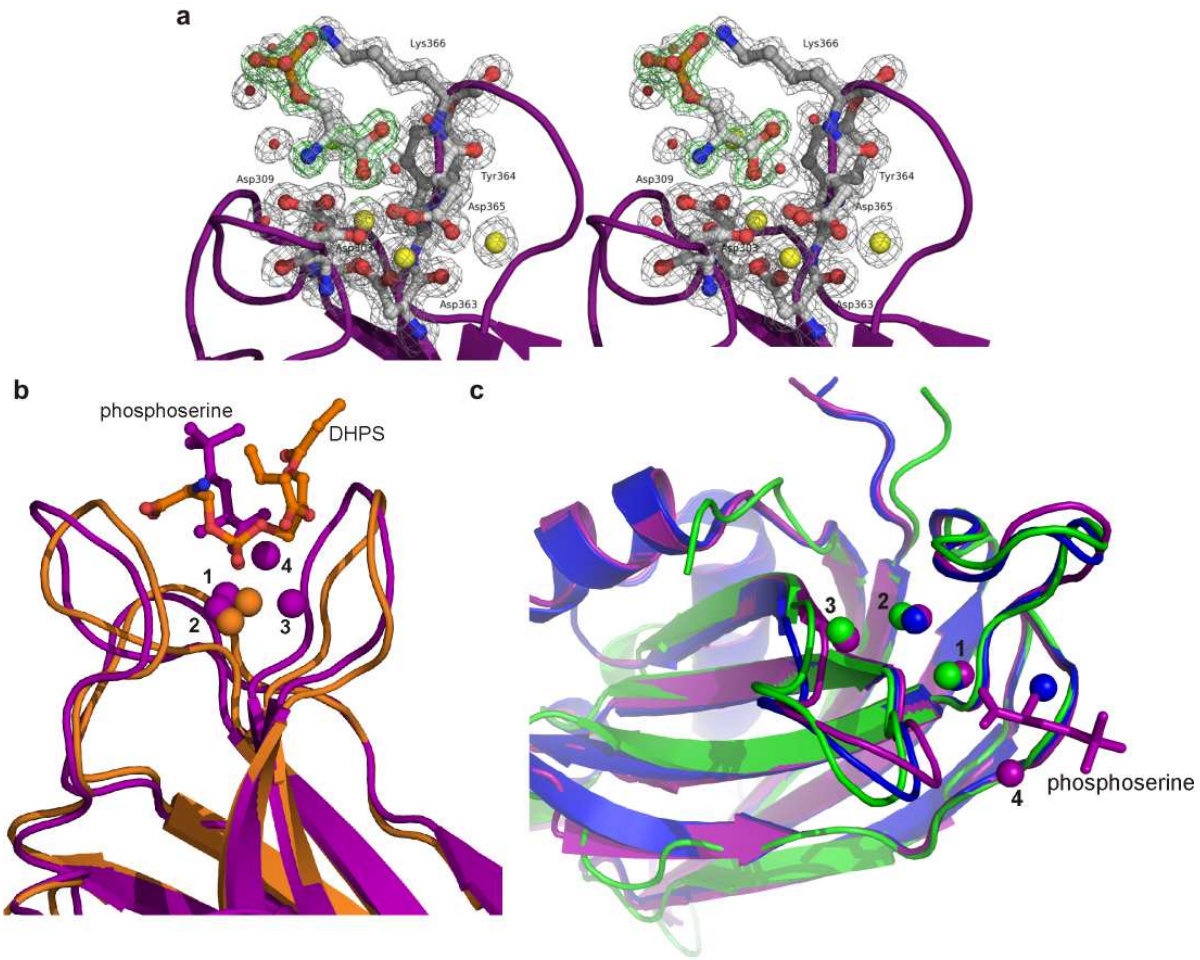

Supplementary Figure 8. Ca^{2+} and PS binding to the C2B-domain of synaptotagmin-1. (**a**) Close-up of the phosphoserine bound Ca^{2+}-binding site of the C2B-domain from synaptotagmin-1 with overlaid electron density maps. The final 1.5 Å-resolution 2mFo-DFc electron density map is contoured at σ = 1.3 and shown in grey. The omit difference mFo-DFc map calculated in the absence of phosphoserine is shown with a contour level of σ = 2.5 (green) at the site of the ligand. (**b**) Overlay of phosphoserine bound C2B-domain of synaptotagmin-1 (this work; purple) with the structure of 1,2-dihexanoyl phosphatidylserine (C6:0; DHPS) bound to the C2-domain of PKCα (pdb: 1DSY; orange)[40]. Note the completely different positions and orientations of the PS-headgroups. Structures superimposed with a root-mean-square deviation of 1.6 Å for the core regions and both proteins share 37.3% sequence identity. Overlay was done with the SSM Superpose tool in COOT[55]. (**c**) Ca^{2+}-binding to the C2B-fragment of synaptotagmin-1. C2B bound to four Ca^{2+}-ions in one of the molecules in our crystal structure (purple). Ca^{2+}-binding to the sites marked 1 and 2 is well established. The third Ca^{2+}-binding site has not been observed previously for the C2B-domain, but is well established for other C2-domains including the low affinity binding site of the C2A-domain (green; pdb: 1BYN) (Shao, *Biochemistry* **37,** 16106 (1998)). Asp232 and Asp238 that stabilize the third Ca^{2+}-ion in the C2A domain are conserved in C2B (Asp365 and Asp371). The fourth Ca^{2+}-binding site has not been observed previously for the C2B-fragment and does not correspond to Ca^{2+} three in the apo-form (blue; pdb: 1UOV)[41], which would clash with the bound phosphoserine. The fourth Ca^{2+}-ion is not coordinated to the protein but can interact with the phosphate group of phosphoserine and Asp309.

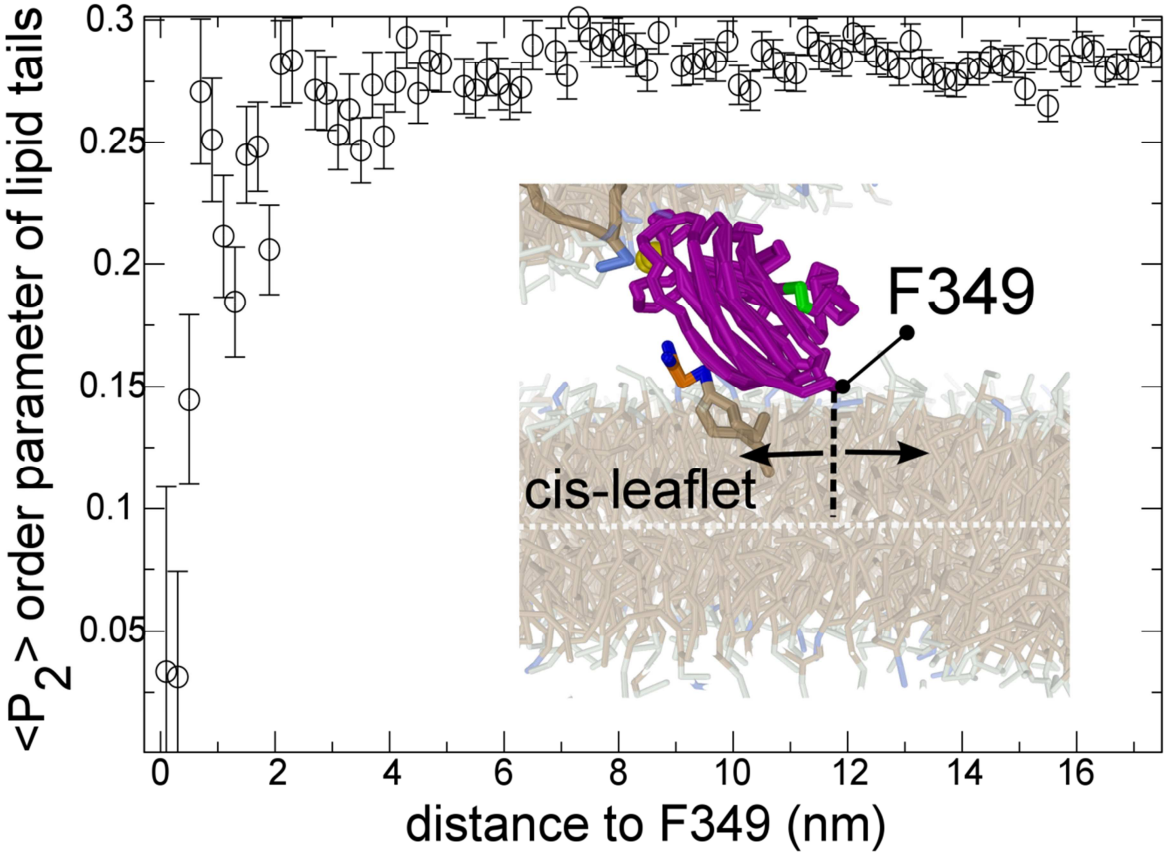

Supplementary Figure 9. Membrane protrusion of the C2B-domain. Molecular dynamics simulation of the 'perpendicular' binding mode of synaptotagmin-1 as in figure 8d. Shown is the (local) second-rank <P2> order parameter of the lipid acyl chains in the lower membrane as function of the distance to residue Phe349, which is the loop that inserted deepest in our simulations. The <P2> order parameter provides a measure for the ordering of the lipid acyl chains with respect to the membrane normal. Perfect alignment with the bilayer normal is indicated by <P2> = 1, perfect anti-alignment by <P2> = -0.5, and a random orientation by <P2> = 0. Reduced values of the <P2> order parameter were observed in close proximity (< 5nm) to Phe349 (*i.e.*, the membrane regions directly under the C2B-domain). The reduced <P2> indicates that the shallow insertion (protrusion) of the (hydrophobic) loop regions of the C2B-domain disorders the packing of nearby lipid acyl chains and thereby causes a local perturbation of the membrane. The values depicted are averages over the consecutive bonds in each lipid acyl chains from the last 100 ns of simulation. The position with respect to Phe349 is determined by the center of mass of the lipid acyl chains.

Supplementary Notes

Sequences of synthetic gene constructs

Sequence of the RQRQ mutant of synaptotagmin-$1_{97–421}$:

```
CATATGGGTGGTAAAAACGCTATCAACATGAAAGACGTTAAAGACCTGGGTAAAACCATGAAAGACCAGGCTCTG
AAAGACGACGACGCTGAAACCGGTCTGACCGACGGTGAAGAAAAAGAAGAACCGAAAGAAGAAGAAAAACTGGGT
AAACTGCAGTACTCTCTGGACTACGACTTCCAGAACAACCAGCTGCTGGTTGGTATCATCCAGGCTGCTGAACTG
CCGGCTCTGGACATGGGTGGTACCTCTGACCCGTACGTTAAAGTTTTCCTGCTGCCGGACAAAAAAAAAAAATTC
GAAACCAAAGTTCACCGTAAAACCCTGAACCCGGTTTTCAACGAACAGTTCACCTTCAAAGTTCCGTACTCTGAA
CTGGGTGGTAAAACCCTGGTTATGGCTGTTTACGACTTCGACCGTTTCTCTAAACACGACATCATCGGTGAATTT
AAAGTTCCGATGAACACCGTTGACTTCGGTCACGTTACCGAAGAATGGCGTGACCTGCAGTCTGCTGAAAAAGAA
GAACAGGAAAAACTGGGTGACATCTGCTTCTCTCTGCGTTACGTTCCGACCGCTGGTAAACTGACCGTTGTTATC
CTGGAAGCTAAAAACCTGAAAAAAATGGACGTTGGTGGTCTGTCTGACCCGTACGTTAAAATCCACCTGATGCAG
AACGGTAAACGTCTGAAAAAAAAAAAAAACCACCATCAAAAAAAACACCCTGAACCCGTACTACAACGAATCTTTC
TCTTTCGAAGTTCCGTTCGAACAGATCCAGAAAGTTCAGGTTGTTGTTACCGTTCTGGACTACGACAAAATCGGT
AAAAACGACGCTATCGGTAAAGTTTTCGTTGGTTACAACTCTACCGGTGCTGAACTGCGTCACTGGTCTGACATG
CTGGCTAACCCGCAGCAGCCGATCGCTCAGTGGCACACCCTGCAGGTTGAAGAAGAAGTTGACGCTATGCTGGCT
GTTAAAAAATAGTAAGAATTC
```

Sequence of C2B (synaptotagmin-$1_{271–421}$):

```
CATATGGAAAAACTGGGTGACATCTGCTTCTCTCTGCGTTACGTTCCGACCGCTGGTAAACTGACCGTTGTTATC
CTGGAAGCTAAAAACCTGAAAAAAATGGACGTTGGTGGTCTGTCTGACCCGTACGTTAAAATCCACCTGATGCAG
AACGGTAAACGTCTGAAAAAAAAAAAAAACCACCATCAAAAAAAACACCCTGAACCCGTACTACAACGAATCTTTC
TCTTTCGAAGTTCCGTTCGAACAGATCCAGAAAGTTCAGGTTGTTGTTACCGTTCTGGACTACGACAAAATCGGT
AAAAACGACGCTATCGGTAAAGTTTTCGTTGGTTACAACTCTACCGGTGCTGAACTGCGTCACTGGTCTGACATG
CTGGCTAACCCGCGTCGTCCGATCGCTCAGTGGCACACCCTGCAGGTTGAAGAAGAAGTTGACGCTATGCTGGCT
GTTAAAAAATAGTAGCTCGAG
```

Fluorescence cross correlation spectroscopy (FCCS)

To study potential oligomerization of C2AB in solution and in the membrane bound state we applied FCCS (Supplementary Fig. 7) (Schwille, *Biophys. J.* **72**, 1878 (1997)). The fluorescence signals of a ~30 nM solution of each of the two potential binding partners (C2AB-AF488 and C2AB-KK114) were recorded independently on two detectors simultaneously. Each channel was auto-correlated and additionally the two channels were cross-correlated. From the autocorrelation curve of each channel the concentrations and diffusion coefficients (which is related to the molecule size) of the potential binding partners were estimated. The amplitude of the cross-correlation curve is related to the amount of oligomerized C2AB-AF488–C2AB-KK114 complexes. In case of binding to supported lipid bilayers (75 mol% DOPC, 15 mol% DOPS), both C2AB-AF488 and C2AB-KK114 were added to the solution to a final concentration of 7 nM C2AB for each color. The focal volume was positioned on the membrane and correlation curves were recorded. To induce membrane binding of the C2AB fragments, 1 mM Ca^{2+} was added to the solution. After 5 min incubation, correlation curves were recorded with the focus again positioned on the membrane. Membrane binding was verified by taking *x-z* images of the bilayer region before and after addition of 1 mM Ca^{2+}. The fluorescence signal was clearly enhanced after Ca^{2+} addition. Additionally, the membrane bound fraction was estimated by fitting the correlation curves obtained in presence of Ca^{2+} with a two component model. Here, the first transit time was fixed to the transit time of C2AB in solution (determined before with an independent measurement). The fit of the correlation curves indicated that ~93% of C2AB was membrane bound. The setup was calibrated for the maximum overlap of the focal volumes for the two channels (488 and 633 nm) by measuring FCCS in a solution (*i.e.* in the absence of a membrane) containing 0.5 nM of two color double stranded DNA (IBA, Göttingen, Germany).

Molecular dynamics simulations

Simulation model and settings

The molecular dynamics simulations were performed with the GROMACS simulation package[57], version 4.5. We used the MARTINI coarse-grained model (reference 42 and Monticelli, *J. Chem. Theory Comput.* **4,** 819 (2008)) to simulate the lipids, amino acids and solvents. Solvent was modeled by a single bead that represented four water molecules. This substantially reduced the size of the simulation system and enabled to study systems

Nature Structural & Molecular Biology: doi:10.1038/nsmb.2570

that were hitherto considered too large for molecular dynamics simulations. In all simulations, the system was coupled to a constant temperature bath (Lopez, *J. Chem. Theory Comput.* **5,** 3195 (2009)) with a relaxation time of 1.0 ps. We performed our simulations at temperatures of 310 K and periodic boundary conditions were applied to simulate bulk behavior. The time step used in the simulation was 20 fs (Risselada, *J. Chem. Phys.* **112,** 7438 (2008)). The neighbor-list was updated every 10 simulation steps. The pressure was weakly coupled (Berendsen, *J. Chem. Phys.* **81,** 3684 (1984)) to 1 bar with a relaxation time of 0.5 ps. In analogy to the other studies done with the MARTINI model, the time scales quoted in this work were scaled by a factor of four to approximately correct for the faster diffusion rates of water and lipids in the coarse-grained model[42].

Modeling phosphoinositides

In our model PIP2 was represented by a coarse-grained mimic[7]. The applied bonded and non-bonded parameters are standard parameters within the MARTINI model[42]. The inositol group in the PIP2 model was included as a triangular ring structure, inspired by a recent parameterized coarse-grained model of glucose (Lopez, *J. Chem. Theory Comput.* **5,** 3195 (2009)), and was formed by three weakly polar beads (MARTINI type P2)[42], representing the presence of the three alcohol groups. To each of these three beads a phosphate group (type Qa) was bound with a charge of -2 for the two free phosphate groups and -1 for the glycerol bound phosphate group. The glycerol group was modeled by two intermediate polar beads (type Na). Connected to the glycerol were a stearoylic and an arachidonic acid, which is the predominant PIP2 species in the brain. The saturated stearoylic acid was modeled by four apolar C1 beads, and the poly-unsaturated arachidonic acid by four slightly less apolar C4 beads. The phosphatidylserine headgroup of DOPS was modeled by two beads: P5 for the neutral serine group and Qa for the negatively charged phosphate group.

Modeling the PIP2–PS–C2B-domain complex.

The C2B-domain of synaptotagmin-1 was modeled based on the X-ray structure of Ca^{2+} and phosphoserine-bound C2B provided in this work. PIP2 was modeled in based on the crystal structure of the C2-domain of PKCα with PIP2[39]. The secondary structure was determined from the pdb file according to the dssp definition. Dihedral restraints between neighboring backbone beads were applied to conserve the dssp derived secondary structure (Monticelli, *J. Chem. Theory Comput.* **4,** 819 (2008)). In addition an elastic network between the backbone beads (based on a 0.5 – 0.9 nm cutoff distance) was applied to conserve the overall structure. The phosphate bead of the PS headgroup and the two calcium atoms were bound to the C2B-domain via an elastic network with the neighboring groups of its binding pocket (based on an 1.0 nm cutoff distance). The equilibrium position of the coarse-grained phosphate headgroup and calcium atoms were derived from the X-ray structure (center of mass based). The same method was applied to attach the PIP2 headgroup. Here, the binding to the C2B-domain was facilitated by an elastic network with the non-free phosphate group of PIP2 (located between the glycerol and inositol group).

Membrane simulations

The ability of the PIP2–PS–C2B-domain complex to dock to a 40 nm synaptic vesicle was first studied by embedding the complex in a 13 × 13 nm planar membrane. Here, the presence of a 40 nm vesicle was mimicked by an external harmonic field. The carbon tails and glycerol of the bound DOPS were kept inside this implicit vesicle via a repulsive potential with its surface. The (outside) surface of this 'vesicle' repelled the atoms of the C2B-domain and the membrane but did not interact with the solvent in the system. This implicit vesicle was placed on various minimal distances from the membrane (0, 1, 2 and 3 nm) to study the partitioning of the PIP2–PS–C2B-domain complex. Because the membrane could freely move with respect to the implicit vesicle (which was fixed in space), an equilibrium state, defined by the absence of visual membrane perturbations, was reached for all starting conditions. Once we had defined the equilibrium state, we replaced the implicit vesicle by the corresponding explicit vesicle (consisting of 7,644 DOPC and 1,348 DOPS lipids) (Risselada, *J. Chem. Phys.* **112,** 7438 (2008)), and replaced the 13 × 13 nm membrane by an 49 × 44 nm membrane (consisting of 5,332 DOPC and 940 DOPS lipids). Sodium counter-ions were added to neutralize the system. This large explicit system was run for an additional 500 ns. The ‘parallel’ membrane binding conformation of the PIP2–PS–C2B-domain complex was studied in a 13 × 13 nm planar membrane and simulated for 1 μs.

Nature Structural & Molecular Biology: doi:10.1038/nsmb.2570